

# Anisotropic Photophysical Properties of Highly Aligned Crystalline Structures of a Bulky Substituted Poly(thiophene)

Yingying Wang,<sup>†,§</sup> Barbara Heck,<sup>†</sup> Daniel Schiefer,<sup>‡</sup> John O. Agumba,<sup>†</sup> Michael Sommer,<sup>‡,§</sup> Tao Wen,<sup>\*,†</sup> and Günter Reiter<sup>\*,†,§</sup>

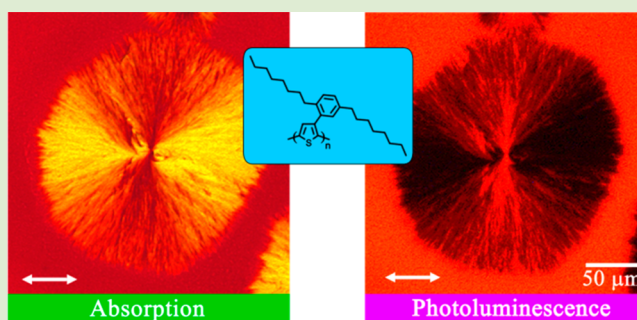
<sup>†</sup>Institute of Physics, University of Freiburg, Herman-Herder-Strasse 3, 79104 Freiburg, Germany

<sup>‡</sup>Institute of Macromolecular Chemistry, University of Freiburg, Stefan-Meier-Strasse 31, 79104 Freiburg, Germany

<sup>§</sup>Material Research Center Freiburg (FMF), Stefan-Meier-Strasse 21, 79104 Freiburg, Germany

## Supporting Information

**ABSTRACT:** The photophysical properties of a phenyl-substituted poly(thiophene), poly(3-(2,5-dioctylphenyl)-thiophene) (PDOPT), were studied as a function of polarization and degree of orientation of the crystalline structure. Under well-chosen controlled conditions, large-sized spherulitic crystals of PDOPT were successfully prepared from the melt. From polarized optical microscopy and X-ray diffraction, the molecular orientation of PDOPT within the spherulite was determined, indicating that the fastest growth direction of the spherulite was the *a*-axis. This implied that crystallization of PDOPT was directed by the packing of the side chains rather than the backbones, which are significantly separated. As the crystalline lamellae were all radially oriented, the local absorbance strongly depended on the polarization of the incoming light. Compared to randomly oriented crystals in a quenched and thus rapidly crystallized sample, PDOPT spherulites displayed red-shifted absorption and emission spectra, combined with a reduced photoluminescence quantum yield. Even for these markedly separated polymer backbones (1.47 nm), the reduced photoluminescence suggests an enhancement of interchain interactions of highly ordered bulky substituted polythiophene induced by crystallization.



The optoelectronic properties of conjugated polymers are of importance for their application in organic electronic devices.<sup>1</sup> These properties are considerably determined by both the conformation of the chain-like molecules (intrachain arrangements of chromophores) and the way these molecules pack in the solid state (interchain arrangements of chromophores). In thin films of conjugated polymers prepared by standard techniques like spin coating, interchain energy transport is usually more rapid than intrachain transport.<sup>2</sup> Thus, the corresponding optoelectronic properties depend sensitively on the extent of interchain interactions.<sup>3</sup> It is widely accepted that interchain interactions in thin films are effectively influenced by chain aggregation and film morphology. Consequently, the relevant photophysical and electronic properties can be controlled by appropriate processing conditions.<sup>4,5</sup>

Most previous studies have focused on conjugated polymers with short backbone stacking distances (<5 Å), such as in alkyl-substituted poly(thiophene)s (P3ATs)<sup>5,6</sup> or poly(phenylenevinylene)s (PPVs).<sup>7,8</sup> In these materials, interchain interactions are mainly determined by the overlap of  $\pi$ -orbitals, i.e.,  $\pi$ - $\pi$  interactions. To control interchain interactions, conjugated polymers with bulky side chains have been developed.<sup>9</sup> Bulky side chains can separate the polymer backbones from each other and thus may have a profound influence on the final

properties of these materials.<sup>9,10</sup> In particular, the separation of main chains can strongly improve the photoluminescence (PL) quantum yield ( $Q_p$ ) of conjugated systems.<sup>11</sup> Up to now, however, only a few reports have discussed the relationships between morphology and optoelectronic properties of conjugated systems having a large main chain separation distance (>1 nm).<sup>10,12–14</sup> For such bulky substituted conjugated polymers,  $\pi$ - $\pi$  interactions should be very weak or completely absent. As a consequence, significant differences in the crystallization behavior and the resulting properties are expected.

We have recently synthesized poly(3-(2,5-dioctyl-phenyl)-thiophene) (PDOPT) having an extremely bulky side chain (Figure 1a) by using Kumada catalyst transfer polycondensation.<sup>15</sup> The weight-average molecular weight ( $M_w$ ) of the PDOPT sample was  $2.8 \times 10^4$  g/mol with a dispersity ( $D = M_w/M_n$ ) of 1.86 (denoted as PDOPT-28). According to a previous report, the bulky side groups significantly separate the main chains of PDOPT by 1.47 nm.<sup>12</sup> Hence,  $\pi$ - $\pi$  interactions should not be possible in PDOPT. In the present study, we

Received: July 7, 2014

Accepted: August 18, 2014

Published: August 20, 2014

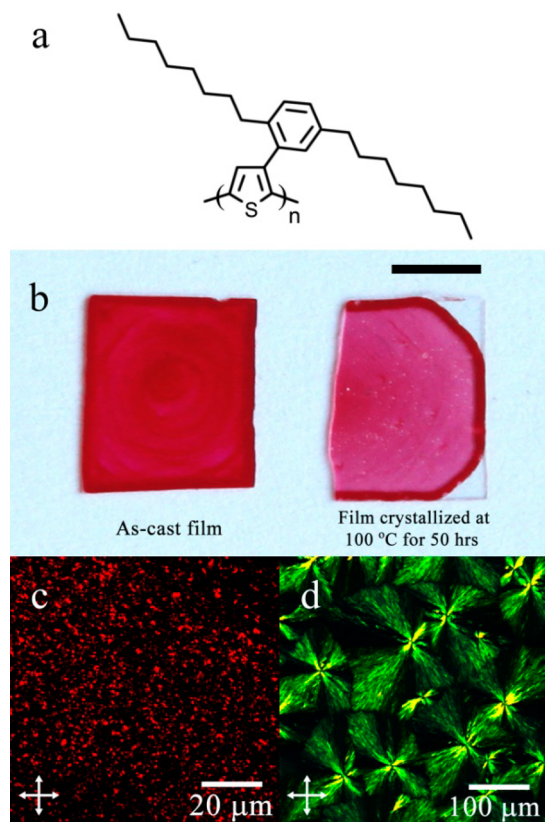


**Figure 1.** (a) Chemical structure of poly(3-(2,5-dioctylphenyl)-thiophene) (PDOPT). (b) Photo of an as-cast and a crystallized film of PDOPT-28 on glass slides (Scale bar: 0.5 cm). Cross-polarized optical micrographs of an as-cast PDOPT-28 film (c) and after isothermal crystallization at 100 °C for 50 h (d). The arrows indicate the orientation of crossed polarizers.

have investigated the influence of this large interchain distance on the crystallization process and examined the corresponding photophysical properties. On the basis of differential scanning calorimetry (DSC) measurements, we concluded that PDOPT could be easily crystallized and melted at temperatures around 47 °C and 113 °C, respectively (Supporting Information, Figure S2a). Interestingly, Aasmundtveit et al. did not observe that PDOPT could be recrystallized.<sup>12</sup> A reason for this difference might be the regioregularity (RR), which was higher in this sample than in that used by Aasmundtveit et al.<sup>12,15</sup> Similar to results obtained for other alkyl-substituted poly(thiophene)s,<sup>16</sup> the DSC curves showed two endothermic peaks. Beckingham et al. ascribed the annealing peak to the formation of distinct amorphous regions,<sup>17</sup> but it seems that the double melting peaks in the present work rather resulted from crystallites with differing melting temperatures. Compared to poly(3-hexylthiophene) (P3HT),<sup>18</sup> the large stacking distance of the polymer chains and the presence of long alkyl side chains are mainly responsible for the about 100 °C lower melting temperature ( $T_m$ ) of PDOPT compared to poly(3-hexylthiophene) (P3HT). As an advantage of this relatively low  $T_m$ , we were able to prepare well-ordered crystalline structures of PDOPT from the melt at much lower temperatures compared to P3HT, avoiding possible thermal degradation.

The crystals of PDOPT were prepared from drop-casted films with a thickness of ca. 1  $\mu\text{m}$  (see Figure S1, Supporting Information) via isothermal crystallization. Intriguingly, after crystallizing a thin film of PDOPT-28 isothermally at 100 °C

for 50 h, the color of the sample became more transparent; i.e., the absorption of light decreased. This could be observed even by the naked eye (Figure 1b). Having a similar thickness, the as-cast film appeared deep red but changed to a less dense rose color after crystallization. The corresponding absorption spectra showed that under nonpolarized light the absorption intensity of spherulites was about 3 times lower than that of disordered crystal grains (Figure S3, Supporting Information). The morphologies of two such samples were observed by an optical microscope under crossed polarizers. Tiny crystals, formed during the fast evaporation of the solvent, were seen in the as-cast film (Figure 1c). In the crystallized sample, however, it was found that large-sized spherulites with diameters of more than 100  $\mu\text{m}$  filled the whole sample. Under crossed polarizers, the spherulites displayed the characteristic Maltese cross optical pattern of radially oriented crystalline lamellae, as revealed by a large birefringence corresponding to a highly preferential orientation of all polymers (Figure 1d).<sup>19</sup> The size of the spherulites widely differed within the same sample, indicating that nucleation did not occur simultaneously and that homogeneous nucleation was the predominant mechanism at this relatively high temperature.<sup>20</sup> The spherulite growth rate of PDOPT-28 at 100 °C was ca. 3  $\mu\text{m}/\text{h}$  (Figure S4, Supporting Information). To the best of our knowledge, this represents the first observation of spherulites of substituted poly(thiophene)s directly obtained from the melt without the guidance of an external factor like a crystallizable solvent (e.g., 1,3,5-trichlorobenzene).<sup>21</sup> Also, the above observation suggests that the color change of the PDOPT-28 film must be attributed to the formation of spherulites.

To investigate the optical properties of PDOPT-28 spherulites in more detail, local optical microscopy on a single spherulite was performed using linearly polarized light by varying the angle  $\Phi$  of the polarizer with respect to the horizontal axis of the images (Figure 2a–c). As a function of  $\Phi$ ,

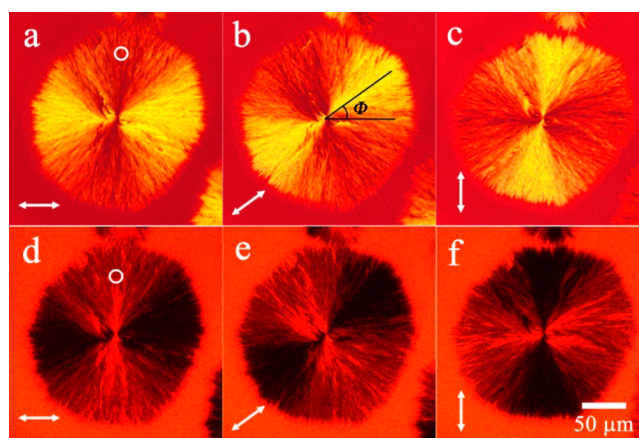


**Figure 2.** Transmission (a–c) and photoluminescence (PL) (d–f) micrographs of a single PDOPT-28 spherulite crystallized at 100 °C for 50 h. The orientation of the polarizer is indicated by arrows.

dark and bright regions within the PDOPT spherulite rotated with  $\Phi$ . These regions arise from strong and weak absorption, corresponding to weak and strong transmittance, respectively. The periodic variation of absorption was correlated with the orientation of the crystalline lamellae within the spherulite relative to the oscillation direction of the linearly polarized incoming light. Sections within the spherulite oriented perpendicular to the polarization direction of the

incoming light displayed intense absorption. The absorption spectra of a PDOPT-28 spherulite measured with polarized light in transmission with a spatial resolution of ca. 8  $\mu\text{m}$  are shown in Figure 3a. The variation of transmission exhibited a

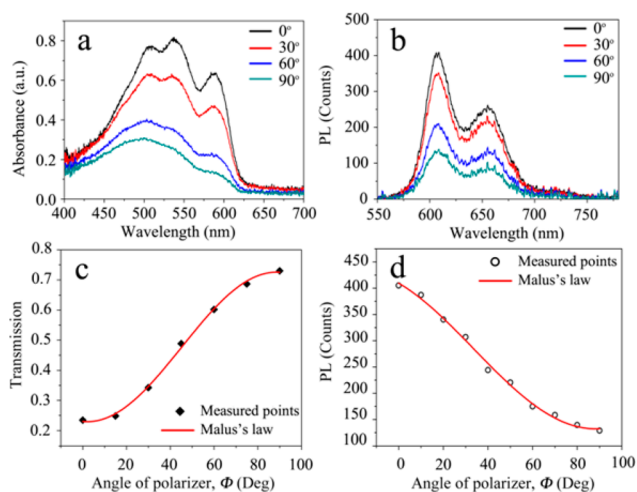


**Figure 3.** Local absorbance (a) and PL (b) spectra of a PDOPT-28 spherulite under polarized light. Absorbance (c) and PL (d) as a function of  $\Phi$  and the corresponding  $\cos^2 \Phi$  fitting. The measured positions within the micrographs are indicated by white rings in Figure 2.

$\cos^2 \Phi$  dependence, in accordance with Malus' law (Figure 3c).<sup>22</sup> This result revealed that the spherulite of PDOPT exhibited an in-plane optical anisotropy with absorption polarization being perpendicular to the radial direction. These observations correspond to the change of color in the crystallized sample shown in Figure 1b. Due to the preferentially oriented lamellar structures, PDOPT spherulites only strongly absorbed the part of the incoming light which was polarized perpendicular to the radial direction of the spherulites. In contrast, the randomly oriented nanoscopic crystalline grains in the as-cast film led to a uniform absorption of light without significant selectivity with respect to polarization direction. As a result, the overall absorbance of the film filled by large spherulites was lower than that of the as-cast film containing a huge number of small and randomly oriented crystallites. The in situ absorption spectra of the two samples shown in Figure 1b as a function of temperature are shown in the Supporting Information, Figure S5. It was found that the amount of light absorbed by PDOPT significantly increased after crystallization from the melt.

The micrographs of Figures 1 and 2 also implied preferential orientation of PDOPT chains within the spherulites. Absorption of polarized light by conjugated molecules is determined by the orientation of their transition dipole moments. For substituted poly(thiophene)s, the transition dipole moment orients along the axis of the main chain of the polymer, i.e., the  $c$ -axis of the crystal unit cell.<sup>23</sup> Clearly, the absorption micrographs indicate that the transition dipole moment ( $c$ -axis) of PDOPT has to be in-plane and along the tangential direction of the spherulite. Accordingly, the PL micrographs (Figure 2d–f) and spectra (Figure 3b) of the same PDOPT-28 spherulite were taken using a polarizer after light was reflected by the sample. These polarized PL micrographs showed a pattern complementary to the absorption images, which indicated that the emitted light from the PDOPT

spherulite was also polarized perpendicular to the radius. Another PDOPT sample with a different  $M_w$  and a narrower  $\mathcal{D}$  was also studied (see Figure S6, Supporting Information). The comparison between the two PDOPT samples revealed that the photophysical properties were largely independent of  $M_w$  and  $\mathcal{D}$ . Of course, the melting and crystallization temperatures, as determined by DSC, depended on  $M_w$  (see Figure S2b, Supporting Information).

The dichroic ratio ( $R$ ) is defined as  $R = A_{\parallel}/A_{\perp}$ , where  $A_{\parallel}$  and  $A_{\perp}$  are the incoming light intensity absorbed by the spherulite having a polarization direction parallel ( $\parallel$ ) and perpendicular ( $\perp$ ) to the PDOPT chain direction, i.e., orthogonal or parallel to the radial axis of the spherulite, respectively. The maximum dichroic ratio of a PDOPT spherulite at the peak absorption wavelength of 587 nm (see Figure 3a) was found to be 4.8. This result is quite similar to the values obtained for highly oriented P3HT films prepared under external driving forces, e.g., strain alignment ( $R = 4.8$ )<sup>24</sup> or mechanical rubbing ( $R = 5.1$ ).<sup>25</sup>

The molecular structure of an isothermally crystallized PDOPT-28 film was also investigated by X-ray diffraction (XRD) (Figure 4a). The diffraction peaks at  $2\theta$  of  $6.0^\circ$  and

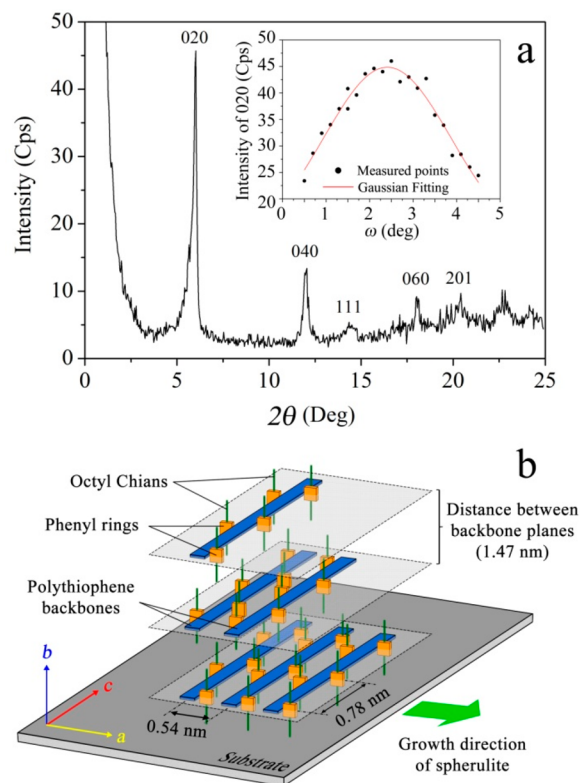


**Figure 4.** (a) XRD pattern of an isothermally crystallized PDOPT-28 film, obtained in reflection mode. Inset: Intensity of the 020 peak as a function of the angle  $\omega$ . (b) Schematic representation of crystalline arrangement of PDOPT chains within a spherulite.

$12.0^\circ$  correspond to 020 and 040 reflections ( $2\theta$  being the scattering angle, for an X-ray wavelength of 0.154 nm). These results indicated that the mean distance between polythiophene backbones was 1.47 nm, consistent with previously investigated films.<sup>12</sup> This supports the idea that the slow crystallization process performed at a comparatively high temperature yielded the same backbone stacking distance of PDOPT as for the sample having lower RR crystallized at room temperature.

To determine the orientation of the lattice planes, additional scattering experiments were performed. Details of the experimental method were introduced in a previous report.<sup>26</sup> In brief, a series of scattering curves were collected at several angles  $\omega$  ( $\omega$  is the angle between the incident beam and the sample surface plane) in the range from  $1.5^\circ$  to  $4.5^\circ$ , varying  $2\theta$  (the angle between the scattered and the incident beam) from  $3^\circ$  to  $9^\circ$  (Figure S7, Supporting Information). The intensities of the 020 peak were plotted as a function of  $\omega$  (Figure 4a, inset), exhibiting a Gaussian distribution. The maximum intensity appeared at around  $\omega = 2.5^\circ$ , which is close to half of the  $2\theta$ -value of the 020 lattice peak position. Accordingly, it could be concluded that the 020 lattice plane was preferentially oriented parallel to the substrate. The same orientation was also observed in a previous work on the as-cast and as-spun PDOPT films with a lower RR.<sup>12</sup> A schematic drawing of the crystal structure and molecular orientation within the spherulite is shown in Figure 4b. The backbones of PDOPT chains within spherulites were lying flat on the substrate, and the stacking direction of backbones ( $b$ -axis) was perpendicular to the substrate plane. Consequently, we conclude that the  $a$ -axis was oriented along the radial direction of the spherulite. This reveals that the preferred growth direction of the spherulites was in the direction of the  $a$ -axis, rather than in the direction of the  $b$ -axis as usually observed for alkyl-substituted poly-(thiophene)s.<sup>27</sup> This growth direction implies that crystallization in PDOPT was driven by the side chains and not the backbones. An in-depth study of the detailed crystallization mechanism of PDOPT is in progress.

As shown above, large-sized and highly ordered crystalline spherulites of PDOPT can be prepared via isothermal crystallization at a comparatively high temperature with respect to the crystallization temperature of PDOPT. Thus, taking advantage of the large size of these crystalline objects, we have explored how such a high degree of ordering influenced the interaction between PDOPT chains and the corresponding spatially resolved optical spectra. For comparison, a PDOPT film with randomly oriented small crystallites was prepared by quenching the sample from the melt state ( $150^\circ\text{C}$ ) to room temperature. The thickness of the quenched film was similar to the crystallized sample with spherulites. Profiting from the highly oriented structure of spherulites, the corresponding optical spectra were measured with polarized light with a polarization direction parallel to the dipole moment ( $c$ -axis) of the polymers within the spherulite. Thus, the local optical spectra were mainly measured with light which was absorbed or emitted from aligned and uniquely oriented lamellae within a spherulite. This means that we excluded light absorbed or emitted by the disordered part crystallized during the quench after isothermal crystallization. Due to the isotropic structure of the quenched film, optical spectra from such disordered regions were measured with nonpolarized light.

Figure 5 shows the absorption and PL spectra of a PDOPT-28 solution and film samples. In the absorption spectrum from a dilute PDOPT-28 solution, one broad peak was observed at around 500 nm, which was attributed to fully dissolved chains exhibiting large disorder. For PDOPT film samples, several vibronic peaks, red-shifted with respect to the solution spectrum, were observed at 500, 535, and 587 nm, respectively. These peaks were ascribed to molecular aggregates exhibiting enhanced interchain interactions. The high-energy absorption peaks of quenched and crystallized samples were strongly overlapping with the absorption peak of the solution spectrum.

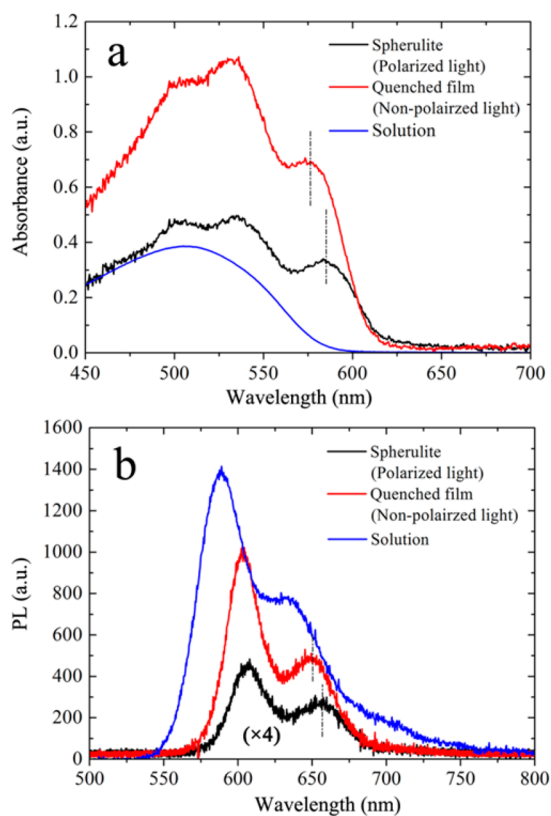


**Figure 5.** Absorbance (a) and PL (b) spectra of spherulite (using polarized light), quenched film (using nonpolarized light), and a dilute solution of PDOPT-28 in *p*-xylene measured at room temperature. (Fluorescence was excited by 450–490 nm light.) The PL spectrum from the spherulite was multiplied by a factor of 4.

This suggests that part of the absorption peak at the lower wavelength may potentially be related to nonaggregated polymers within the film. Moreover, crystallization of PDOPT led to a less pronounced red shift (ca. 80 nm) in the absorption spectrum, compared to P3HT (ca. 160 nm).<sup>28</sup> Tentatively, this could be attributed to a much weaker interchain coupling in PDOPT compared to P3HT.

Comparison of spectra from a quenched film with that from a PDOPT spherulite displayed a small red shift (ca. 10 nm) for the latter, visible in both absorption and PL spectra. A possible interpretation suggests a longer conjugation length for polymers in the spherulite compared to those in the small crystallites of the quenched film. Slow kinetics of crystallization at high temperature most likely allowed for a high degree of molecular ordering and a small number of structural defects. It was found that the quantum yield ( $Q_y$ ) of spherulites did not increase with conjugation length but rather decreased instead. The results derived from Figure 5 indicate that the  $Q_y$  in the highly ordered spherulite was about 50% lower than that in the rather disordered quenched film. This implied that more excitation energy was dissipated in the ordered crystal of PDOPT, via, e.g., electronic energy transfer (EET) between nearby chromophores.<sup>29</sup> A reason for this might be an increase of interchain interactions in PDOPT spherulites due to the better electronic coupling between poly(thiophene) backbones compared to a quenched film.<sup>30</sup> Such higher interchain interaction may have enhanced the migration of excitons to regions of lower energy before having a chance of emitting photons.<sup>31</sup> Similar results were also obtained for other

conjugated polymers with small interchain distance, like P3AT<sup>32</sup> or PPVs,<sup>33</sup> where strong interchain coupling is dominated by  $\pi$ - $\pi$  interactions. Our results strongly suggest that interchain interactions may play a role even for conjugated polymers with large stacking distances, probably due to Coulombic interactions acting over a long range between transition dipoles (Förster resonance energy transfer).<sup>34,35</sup> Our results also suggest that morphological ordering indeed affects photophysical properties of bulky substituted conjugated polymers, which are of potential interest for photoelectronic applications.

In summary, the presence of the bulky side groups in PDOPT weakened interchain cohesion and led to melting at a much lower temperature compared to P3HT. Thus, large-sized and highly ordered crystals of these phenyl-substituted poly(thiophene)s could be prepared simply via isothermal crystallization. The formation of highly ordered structures significantly reduced the overall absorbance due to the selective light absorption of oriented lamellae. This finding provides a potential way for preparing semiconductor layers with a selectable and switchable transmittance. Our spectroscopic results demonstrate that improved molecular ordering can enhance the interchain interactions of conjugated polymers over a large distance and lower the quantum yield.

## ■ ASSOCIATED CONTENT

### 📄 Supporting Information

Methods, detailed experimental procedures, additional data. This material is available free of charge via the Internet at <http://pubs.acs.org>.

## ■ AUTHOR INFORMATION

### Corresponding Authors

\*E-mail: tao.wen@physik.uni-freiburg.de (T.W.).

\*E-mail: guenter.reiter@physik.uni-freiburg.de (G.R.).

### Author Contributions

The manuscript was written through contributions of all authors. All authors have given approval to the final version of the manuscript.

### Notes

The authors declare no competing financial interest.

## ■ ACKNOWLEDGMENTS

We acknowledge funding support from the German Science Foundation (IRTG Soft Matter Science (GRK 1642) and RE 2273/6-1). D.S. and M.S. are grateful to DFG (SPP1355) and the Fonds der chemischen Industrie for funding.

## ■ REFERENCES

- (1) Li, R. J.; Hu, W. P.; Liu, Y. Q.; Zhu, D. B. *Acc. Chem. Res.* **2010**, *43*, 529–540.
- (2) Schwartz, B. J.; Nguyen, T. Q.; Wu, J. J.; Tolbert, S. H. *Synth. Met.* **2001**, *116*, 35–40.
- (3) Schwartz, B. J. *Annu. Rev. Phys. Chem.* **2003**, *54*, 141–172.
- (4) Niles, E. T.; Roehling, J. D.; Yamagata, H.; Wise, A. J.; Spano, F. C.; Moule, A. J.; Grey, J. K. *J. Phys. Chem. Lett.* **2012**, *3*, 259–263.
- (5) Brown, P. J.; Thomas, D. S.; Köhler, A.; Wilson, J. S.; Kim, J.-S.; Ramsdale, C. M.; Sringhaus, H.; Friend, R. H. *Phys. Rev. B* **2003**, *67*, 064203.
- (6) Koch, F. P. V.; Heeney, M.; Smith, P. J. *Am. Chem. Soc.* **2013**, *135*, 13699–13709.
- (7) Qin, T.; Troisi, A. *J. Am. Chem. Soc.* **2013**, *135*, 11247–11256.

- (8) Kohler, A.; Hoffmann, S. T.; Bassler, H. *J. Am. Chem. Soc.* **2012**, *134*, 11594–11601.
- (9) R. Andersson, M.; Thomas, O.; Mammo, W.; Svensson, M.; Theander, M.; Inganäs, O. *J. Mater. Chem.* **1999**, *9*, 1933–1940.
- (10) Theander, M.; Inganäs, O.; Mammo, W.; Olinga, T.; Svensson, M.; Andersson, M. R. *J. Phys. Chem. B* **1999**, *103*, 7771–7780.
- (11) McQuade, D. T.; Kim, J.; Swager, T. M. *J. Am. Chem. Soc.* **2000**, *122*, 5885–5886.
- (12) Aasmundtveit, K. E.; Samuelsen, E. J.; Mammo, W.; Svensson, M.; Andersson, M. R.; Pettersson, L. A. A.; Inganäs, O. *Macromolecules* **2000**, *33*, 5481–5489.
- (13) Andersson, M. R.; Mammo, W.; Olinga, T.; Svensson, M.; Theander, M.; Inganäs, O. *Synth. Met.* **1999**, *101*, 11–12.
- (14) Pan, C.; Sugiyasu, K.; Wakayama, Y.; Sato, A.; Takeuchi, M. *Angew. Chem., Int. Ed.* **2013**, *52*, 10775–10779.
- (15) Schiefer, D.; Wen, T.; Wang, Y.; Goursot, P.; Komber, H.; Hanselmann, R.; Braunstein, P.; Reiter, G.; Sommer, M. *ACS Macro Lett.* **2014**, *3*, 617–621.
- (16) Ho, V.; Boudouris, B. W.; Segalman, R. A. *Macromolecules* **2010**, *43*, 7895–7899.
- (17) Beckingham, B. S.; Ho, V.; Segalman, R. A. *ACS Macro Lett.* **2014**, *3*, 684–688.
- (18) Kohn, P.; Huettner, S.; Komber, H.; Senkovskyy, V.; Tkachov, R.; Kiri, A.; Friend, R. H.; Steiner, U.; Huck, W. T. S.; Sommer, J.-U.; Sommer, M. *J. Am. Chem. Soc.* **2012**, *134*, 4790–4805.
- (19) Shtukenberg, A. G.; Punin, Y. O.; Gunn, E.; Kahr, B. *Chem. Rev.* **2011**, *112*, 1805–1838.
- (20) Wunderlich, B. *Macromolecular Physics*; Academic Press: New York and London, 1976; Vol. 2.
- (21) Müller, C.; Aghamohammadi, M.; Himmelberger, S.; Sonar, P.; Garriga, M.; Salleo, A.; Campoy-Quiles, M. *Adv. Funct. Mater.* **2013**, *23*, 2368–2377.
- (22) Torres-Zuniga, V.; Castaneda-Guzman, R.; Jesus Perez-Ruiz, S.; Morales-Saavedra, O. G.; Zepahua-Camacho, M. *Opt. Express* **2008**, *16*, 20724–20733.
- (23) Gurau, M. C.; Delongchamp, D. M.; Vogel, B. M.; Lin, E. K.; Fischer, D. A.; Sambasivan, S.; Richter, L. J. *Langmuir* **2006**, *23*, 834–842.
- (24) O'Connor, B.; Kline, R. J.; Conrad, B. R.; Richter, L. J.; Gundlach, D.; Toney, M. F.; DeLongchamp, D. M. *Adv. Funct. Mater.* **2011**, *21*, 3697–3705.
- (25) Heil, H.; Finnberg, T.; von Malm, N.; Schmechel, R.; von Seggern, H. *J. Appl. Phys.* **2003**, *93*, 1636–1641.
- (26) Jahanshahi, K.; Botiz, I.; Reiter, R.; Thomann, R.; Heck, B.; Shokri, R.; Stille, W.; Reiter, G. *Macromolecules* **2013**, *46*, 1470–1476.
- (27) Brinkmann, M. *J. Polym. Sci., Part B: Polym. Phys.* **2011**, *49*, 1218–1233.
- (28) Clark, J.; Silva, C.; Friend, R. H.; Spano, F. C. *Phys. Rev. Lett.* **2007**, *98*, 206406.
- (29) Hwang, I.; Scholes, G. D. *Chem. Mater.* **2010**, *23*, 610–620.
- (30) Park, K. C.; Levon, K. *Macromolecules* **1997**, *30*, 3175–3183.
- (31) Jenekhe, S. A.; Osaheni, J. A. *Science* **1994**, *265*, 765–768.
- (32) Boudouris, B. W.; Ho, V.; Jimison, L. H.; Toney, M. F.; Salleo, A.; Segalman, R. A. *Macromolecules* **2011**, *44*, 6653–6658.
- (33) Lee, T. W.; Park, O. O. *Adv. Mater.* **2000**, *12*, 801–804.
- (34) Förster, T. *Discuss. Faraday Soc.* **1959**, *27*, 7–17.
- (35) Andrew, T. L.; Swager, T. M. *J. Polym. Sci., Part B: Polym. Phys.* **2011**, *49*, 476–498.